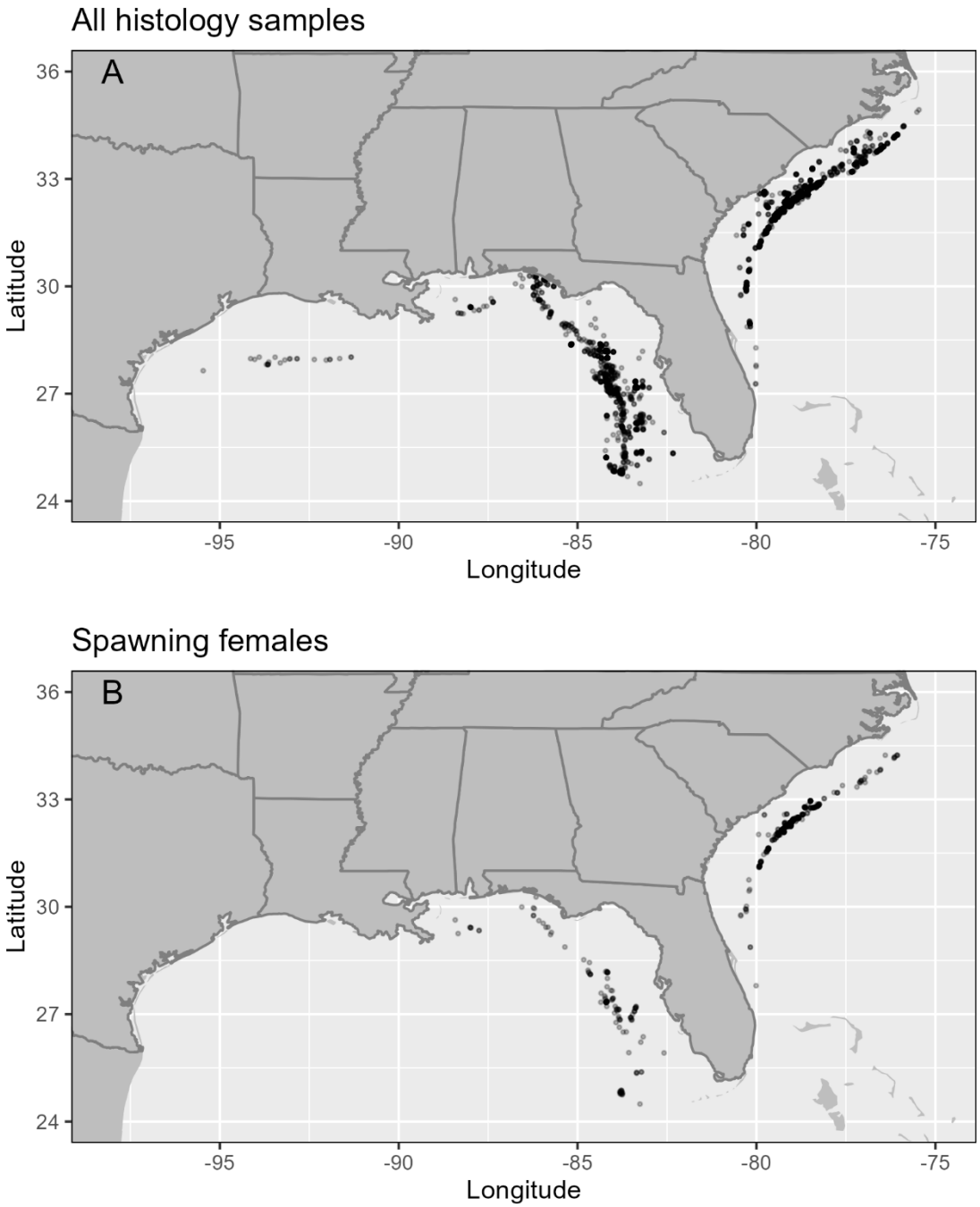

Figure S1: Locations of all scamp histology samples (A) and spawning females (B).

Table S1: Number of histology samples in each region from fishery independent and fishery dependent sources. Years marked with an asterisk (*) were excluded from analyses because they had fewer than 30 total samples.

	US Atlantic				US Gulf of Mexico			
	Fishery Independent		Fishery Dependent		Fishery Independent		Fishery Dependent	
	Spawning	Not Spawning	Spawning	Not Spawning	Spawning	Not Spawning	Spawning	Not Spawning
Total	312	1909	218	1270	26	155	110	1183
1977*	0	0	0	0	0	0	0	14
1978	0	0	0	0	1	6	6	220
1979	0	0	0	62	0	0	20	282
1980	0	17	0	37	0	0	15	131
1981*	0	2	0	6	0	0	0	0
1982*	0	2	0	0	0	0	0	0
1983*	0	6	0	1	0	0	0	0
1984*	2	8	0	0	0	0	0	0
1985*	4	8	0	0	0	0	0	0
1986*	4	3	0	0	0	0	0	0
1987*	1	6	0	0	0	0	0	0
1988	8	22	0	0	0	0	0	0
1989*	5	11	0	0	0	0	0	0
1990	20	55	0	0	0	0	0	0
1991	0	55	0	0	0	0	0	0
1992	10	48	0	0	0	0	0	0
1993	28	56	0	0	0	0	0	0
1994	29	99	0	0	0	0	0	0
1995	6	111	46	13	0	0	0	0
1996	20	126	69	294	0	0	0	0
1997	1	193	0	0	0	0	0	0
1998	32	74	0	0	0	0	0	0
1999	2	65	0	0	0	0	0	0
2000	10	55	0	0	5	18	0	0
2001	5	91	0	0	0	9	0	0
2002	2	57	0	0	5	12	1	8
2003	0	53	0	0	0	0	0	0
2004	17	60	0	4	1	17	4	40
2005	7	68	0	428	1	13	24	143
2006	1	39	66	276	0	0	0	0
2007	2	87	37	144	0	18	0	8
2008	0	20	0	0	1	6	4	10
2009	2	37	0	0	0	12	0	0
2010	13	29	0	0	8	0	0	2
2011	14	60	0	0	1	4	0	9
2012	14	52	0	5	1	3	29	122
2013	21	39	0	0	2	9	5	146
2014	15	78	0	0	0	6	0	23
2015	14	63	0	0	0	6	1	18
2016	3	54	0	0	0	9	1	7
2017*	0	0	0	0	0	7	0	0

Text S1 – Position Relative to the Shelf Break

Because we are trying to estimate the distribution of a species that spans both sides of the Florida peninsula, latitude and longitude are not useful as spatial predictors of presence or abundance. For example, the same latitude exists on both the east and west coast of Florida, but the spatial patterns of the scamp are very different on either side of the peninsula. Therefore, if we tried to use latitude to predict scamp presence or abundance, the model would have trouble defining a relationship and would likely provide poor estimates everywhere. Instead, it is more helpful to define position relative to where the continental shelf begins to drop off very quickly (the shelf-break), an ecologically relevant geological feature that follows the coastline throughout the region. Scamp are thought to spawn and be more abundant close to the shelf-break. So, for our analyses we used position relative to the shelf-break instead of latitude and longitude. Specifically, for each location of interest we calculated the distance to the shelf-break and the position along it. We then used these two metrics to define position during our modeling.

To do this, we extracted the 250-meter isobath from GEBCO because it provides a good approximation of the shelf-break in our region (Figure S2). Then, for each location of interest we calculated the distance to the closest point along the shelf-break. Next, we calculated the distance travelling along the shelf break between the USA-Mexico border and that same closest point. In this way, we can define the position of any location in terms of proximity to the shelf-break and position along it (Figure S3). For position along the shelf-break low values indicate locations close to Mexico and high values indicate locations close to North Carolina. When modeling the probability of spawning we only used distance to the shelf-break and not position along it because we had few data points west of Florida. When modeling scamp presence and abundance we used both distance to the shelf-break and position along it to predict the spatial distribution of scamp.

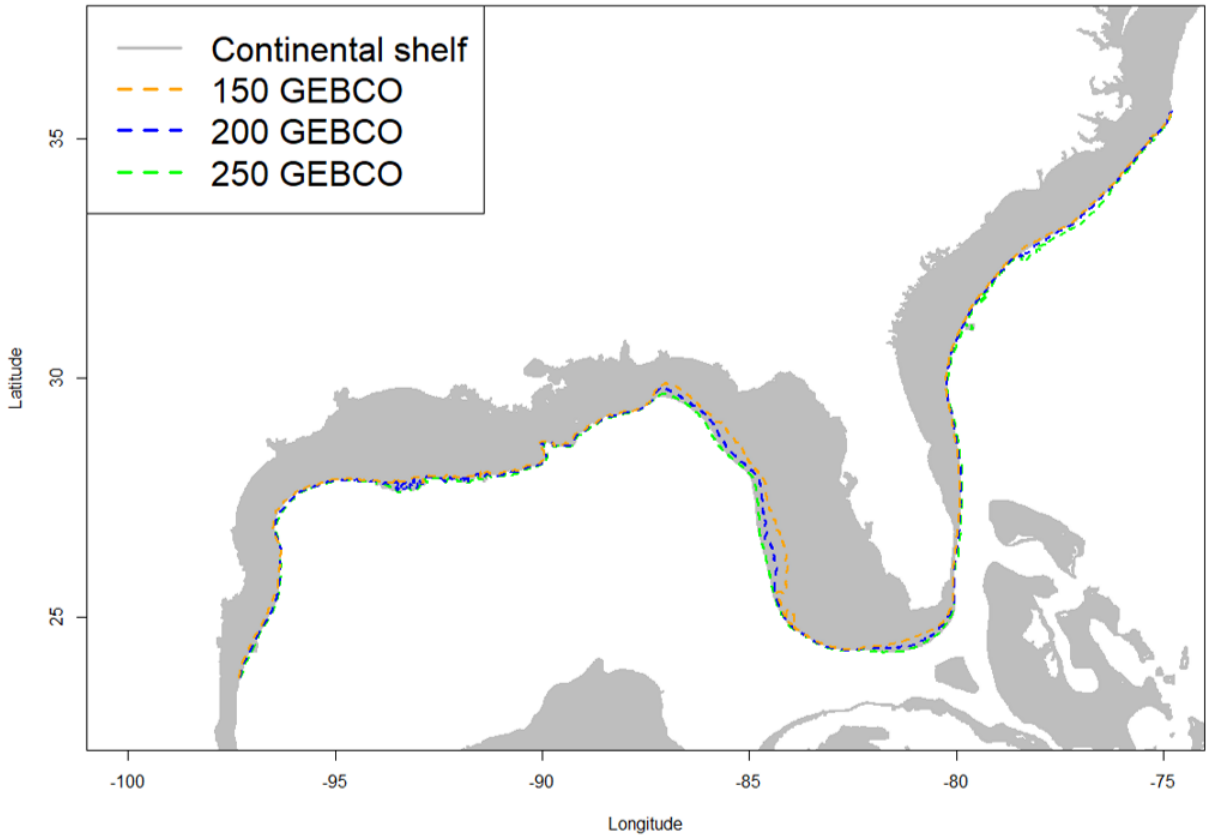

Figure S2: Continental shelf with depth contours. In this region, the 250-meter depth contour closely approximates the outer edge of the continental shelf. Spatial information for the continental shelf is from the Global Seafloor Geomorphic Features map.

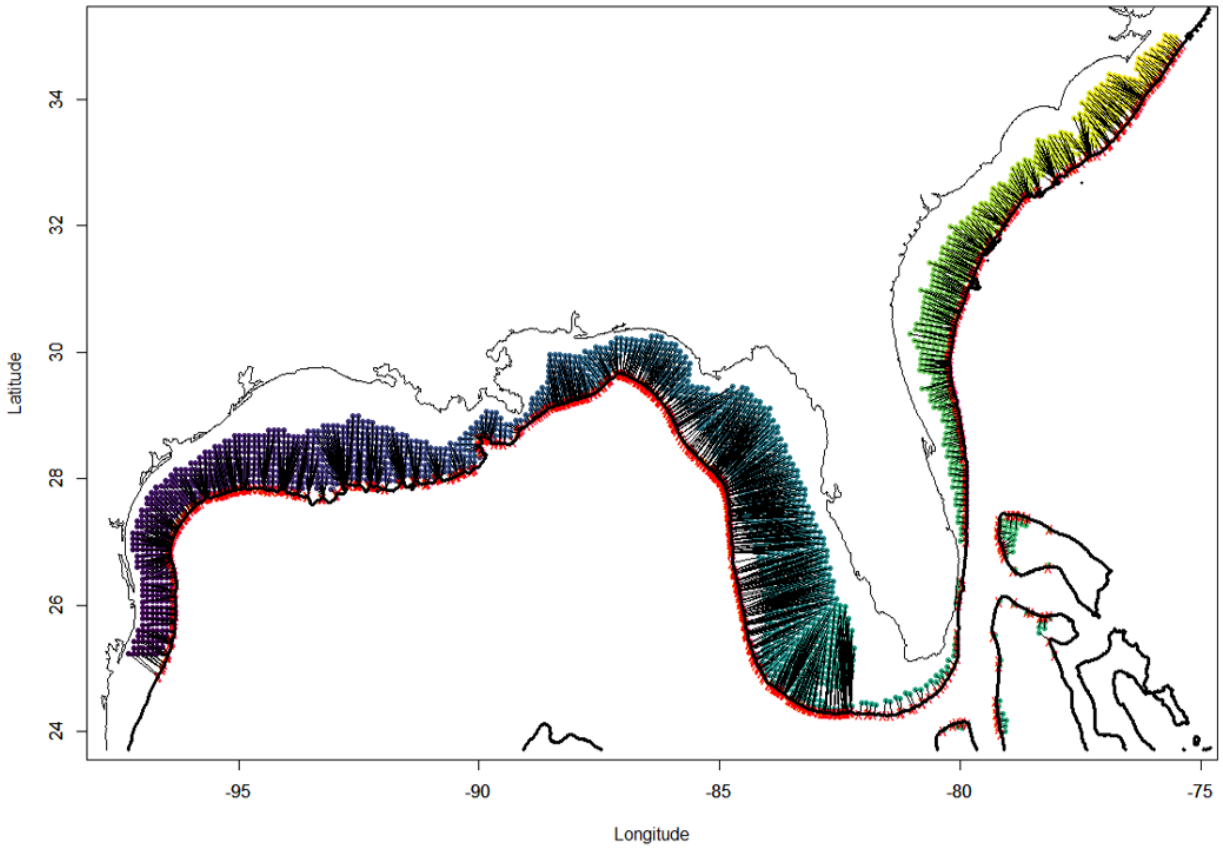

Figure S3: Position relative to the continental shelf-break (250m isobath). To predict the scamp spawning distribution, we defined position relative to the continental shelf-break (thick black line). For each location we calculated the distance (black lines) to the closest point on the shelf-break (red x's). Next, we calculated the distance travelling along the shelf break from the USA-Mexico border and that same closest point. In this way, we can define the position of any location in terms of proximity to the shelf-break and position along it. For position along the shelf-break low values indicate locations close to Mexico (purple points) and high values indicate locations close to North Carolina (yellow points).

Text S2 – Scamp Distribution: Data and Models

Visual Survey Data

To define the spatial distribution of scamp we used data from five fishery independent visual surveys that sample near the southeast United States (Figure S4). This includes four video surveys (FWRI, NMFS-MS, NMFS-PC, SEFIS) and one diver survey (RVC). Although each survey focuses primarily on a different region, there is considerable spatial overlap between them. All three video surveys that sample in the Gulf of Mexico overlap (FWRI, NMFS-MS, NMFS-PC). The diver survey (RVC), which samples in the Florida Keys overlaps with the FWRI video survey. The FWRI video survey also has limited sampling along the east coast of Florida, and therefore overlaps with the video survey off the Atlantic coast of the southern United States (SEFIS). We only used data collected between the years 2011 and 2017 because not all surveys sampled outside of this range.

Three of the four video survey programs quantified scamp abundance using the max N metric (FWRI, NMFS-MS, NMFS-PC), which is the highest number of individuals observed at any single time point during an entire video (Campbell et al. 2015). This is sometimes also referred to as mincount because it represents the minimum estimate of how many fish are present at the site. The fourth video survey (SEFIS), however, uses the sum count (or the associated mean count) metric. This is the sum (or mean) of the number of fish observed on 41 frames throughout the video (Schobernd et al. 2014). Although both metrics have merits, in order to compare the data across surveys we used the individual frame counts from the SEFIS data to calculate an estimated max N as the maximum number of scamp observed on a single frame. Although this is not a true max N, because SEFIS videos are only read for 41 frames rather than the full video, evidence suggests that analysis of limited frames can closely approximate analysis of the entire video (Bacheler and Shertzer 2015).

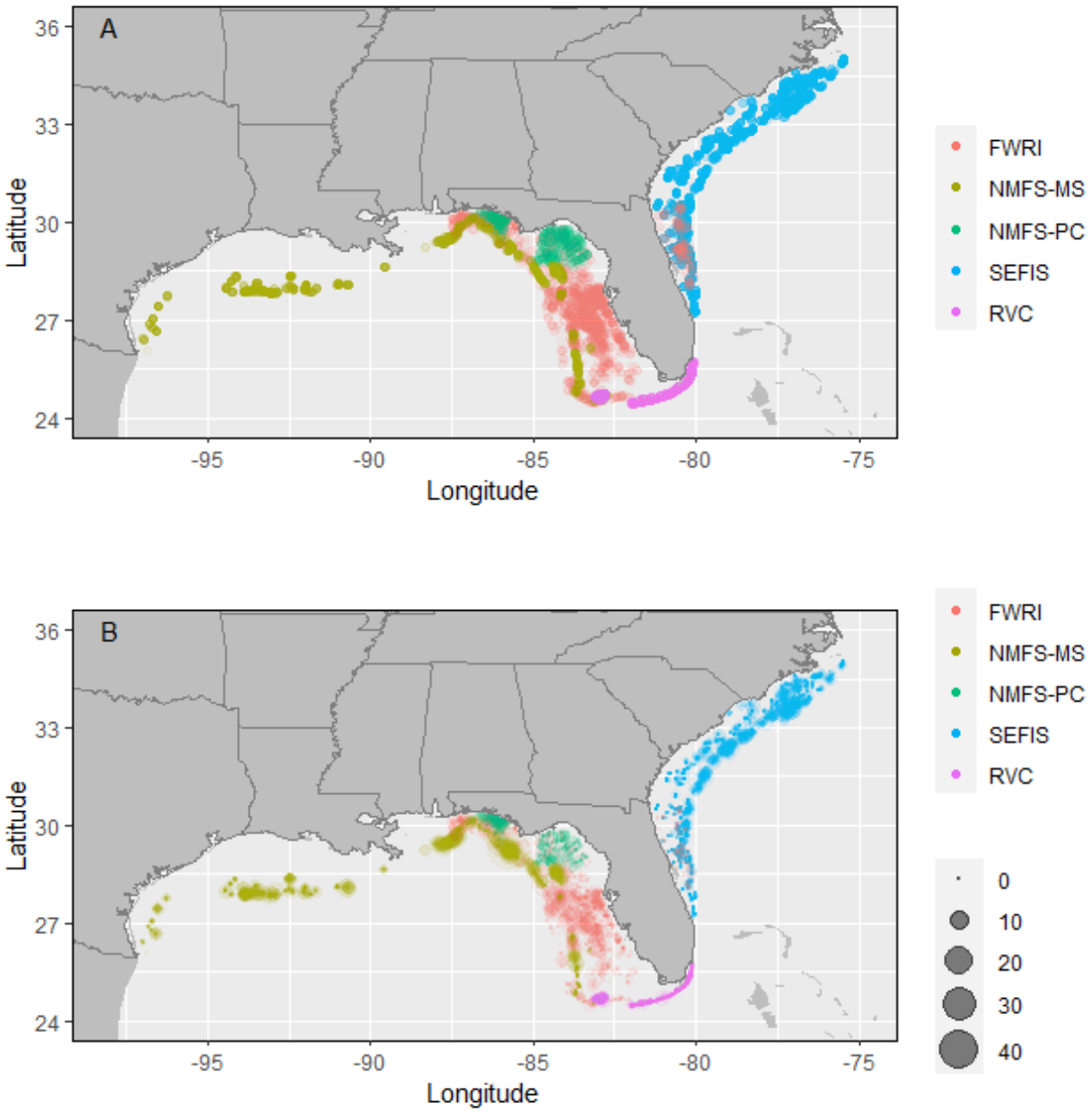

Figure S4: Fishery independent visual survey locations near the southeastern United States. (A) Survey locations sampled by each program, and (B) the same locations with the size of the point scaled by the number of scamp observed.

Visual Survey Delta GAM

We predicted the spatial distribution of scamp by analyzing these visual survey data with a two-step delta GAM approach. First, we developed a binomial GAM sub-model to predict the probability of scamp presence. Next, we used only those survey data that observed scamp to develop an additional GAM sub-model that predicts scamp abundance when present. Then, we estimated the overall abundance of scamp at each release location as the product of these two predictions.

Both sub-models used the same set of covariates, which included all variables that overlap across all five surveys. These are average bottom depth, change in bottom depth, distance to the shelf break and position along the shelf break (Text S1), percent observed substrate, maximum relief, year, and survey program. To standardize across the surveys, we calculated the percent observed substrate as the percent of the bottom that is covered by rock, hard coral, or soft coral. We also sorted relief into three levels; we categorized locations with a maximum relief less than 0.3 meters as "low relief," locations with a maximum relief between 0.3 and 1.0 meters as "moderate relief," and locations with a maximum relief greater than 1.0 meter as "high relief."

For variable selection we used the "select == TRUE" argument in the mgcv package in R, which is the recommended method for GAMs (Marra & Wood 2011) and did not eliminate any covariates for either submodel. Therefore, both final submodels included the entire suite of covariates that overlap across the surveys. The binomial GAM submodel that predicted probability of scamp presence explained 25.6% of the deviance in whether a survey observed scamp and had an adjusted r^2 of 0.238. For the positive count submodel we considered various error distributions, including Gaussian with a fourth root or log transformation, Tweedie, Quasipoisson, Gamma, and Negative Binomial. The Gaussian error distribution with fourth root transformed scamp counts performed the best (based on AIC) and explained 26.2% of the deviance in survey counts (when scamp were observed) and had an adjusted r^2 of 0.254.

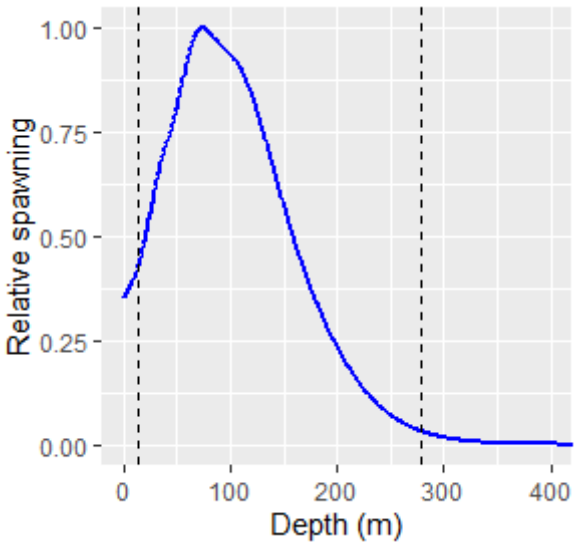

Figure S5: Predicted spawning distribution by depth. Calculated as the product of three models: 1) the probability of scamp presence, 2) the estimated abundance when present, 3) the probability of spawning. Values are proportional to the maximum predicted spawning. We only simulated spawning between depths 14 and 279 (dashed lines), which bound the middle 95% of the area under the depth marginal effect. Empirical histology samples from spawning females ranged in depth from 14 to 177 meters.

Text S3 – Sample Size Selection

To determine how many particles to release in each simulation year we conducted a preliminary set of releases from all locations and dates in three different years. From the results of each year, we subsampled particles with replacement 15 times for each of 80 subsample sizes ranging approximately from 2,000 to 180,000. For each subsample we calculated several proportions of interest (e.g., the proportion of Atlantic recruits that started in the Gulf of Mexico), and the standard deviation of each proportion for a given sub-sample size. We then used plots showing how these proportions and standard deviations change with increasing sub-sample size (Figure S6) to determine that we would not benefit from releasing more than 100,000 particles in a year.

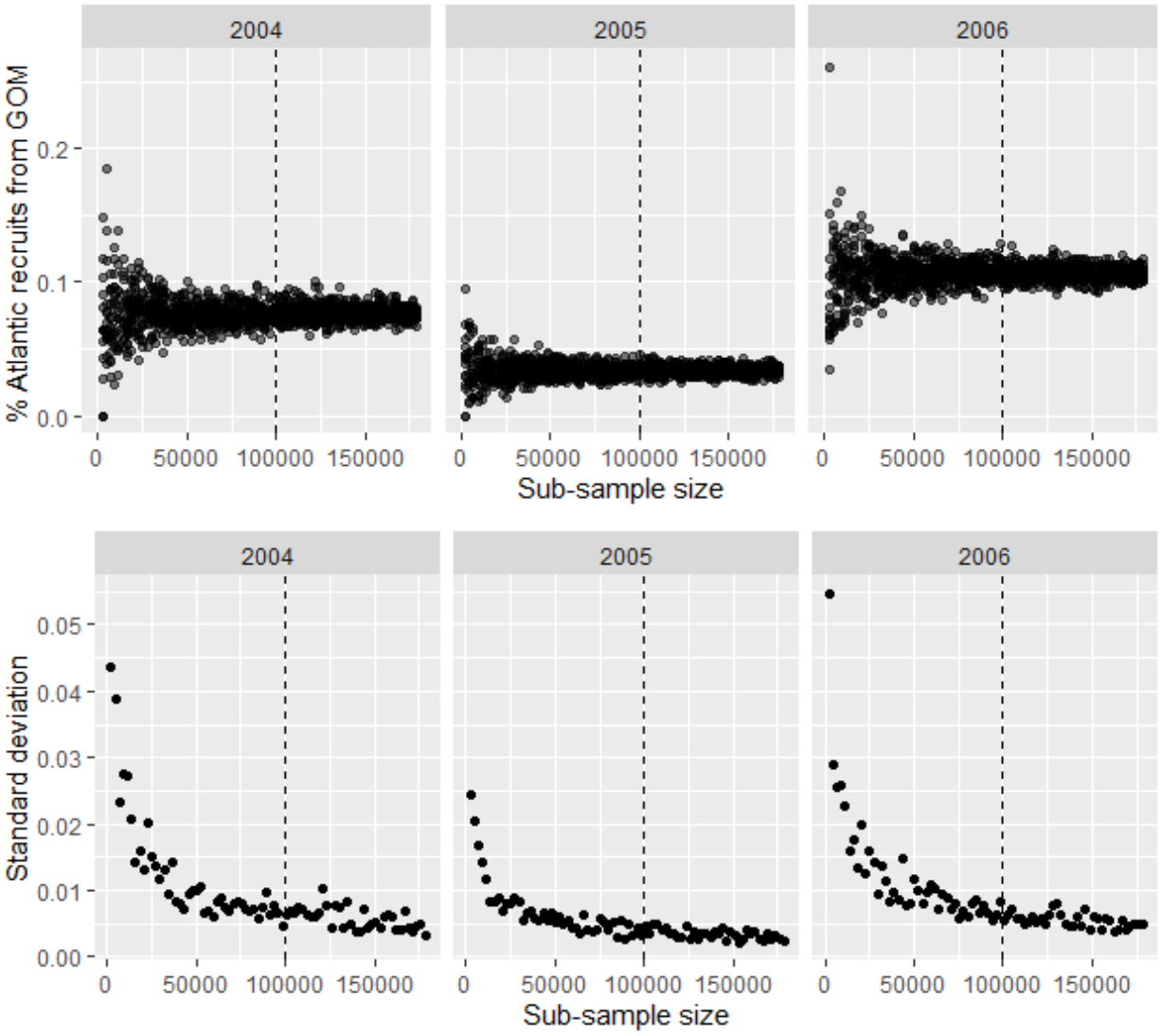

Figure S6: Re-sampling analysis using preliminary simulation results confirmed that 100,000 virtual larvae per year is a sufficient sample size. We took re-samples of various sizes for each of three years. The top row shows the proportion of Atlantic recruits that came from the Gulf of Mexico and the bottom row shows the standard deviation in that proportion for a given sub-sample size.

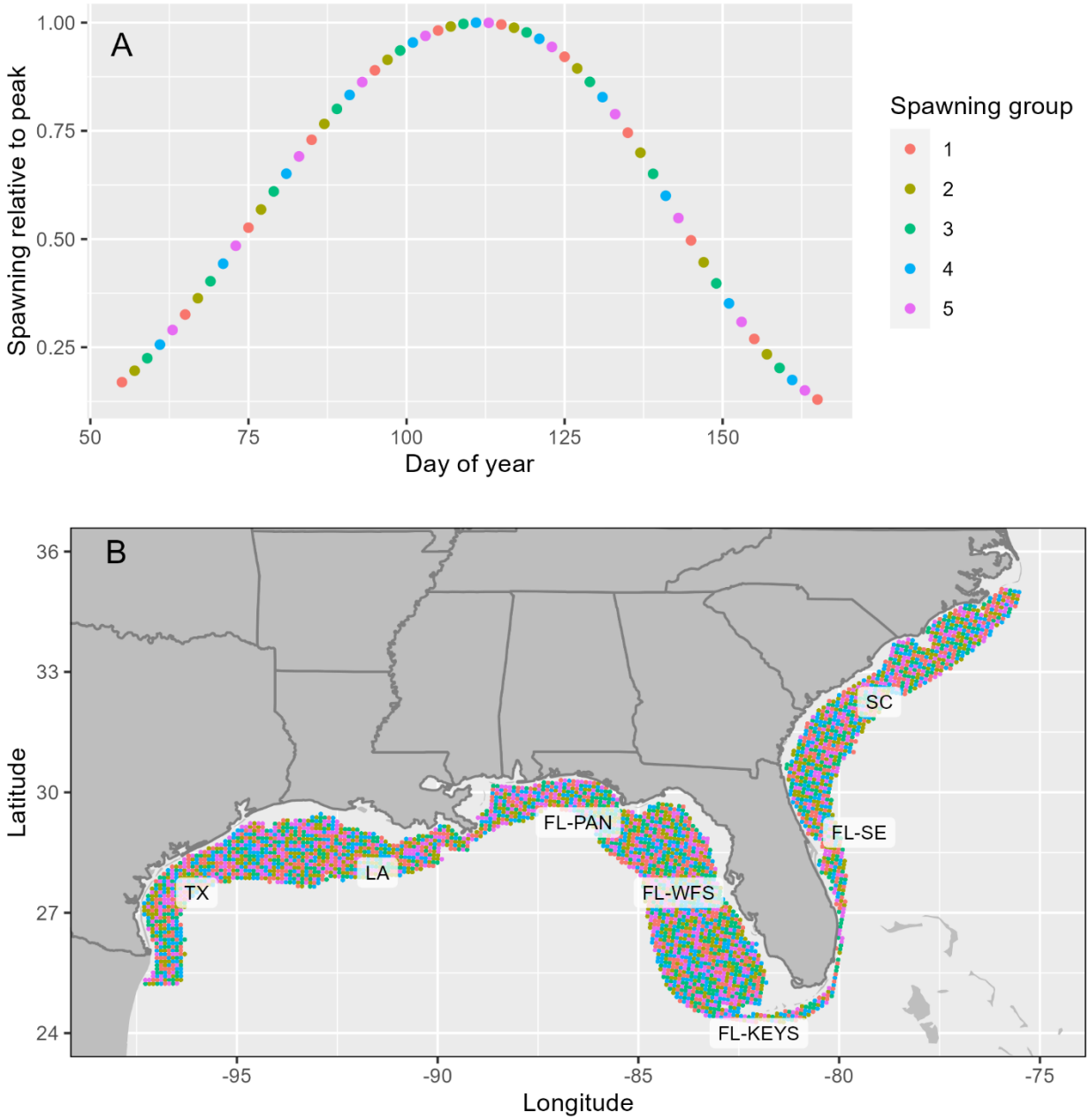

Figure S7: We simulated spawning every other day during the spawning season (A) from grid locations spaced at 10km intervals (B). However, we randomly assigned each location to one of five groups and spawned eggs from each group on a different set of dates. Thus, 20% of the locations simulated spawning on each day, with spawning occurring at individual locations every 10 days. This maintained the temporal and spatial resolution needed for robust probabilistic results but reduced the total number of virtual eggs required for each simulation. The text labels identify the geographic sub-regions referenced in Figures 2 and S10. TX = Texas, LA = Louisiana, FL-Pan = the Florida Panhandle, FL-WFS = the West Florida Shelf, FL-Keys = the Florida Keys, FL-SE = the Atlantic coast of Florida, SC = South Carolina.

Text S4 – Vertical Distribution of Eggs and Larvae

Egg Buoyancy

Because grouper eggs are positively buoyant (Colin et al. 1996), we specified that simulated eggs will float to the surface over the first nine hours and concentrate in the top 15 meters of the water column until 48 hours after release. To define rates of vertical movement that realistically approximate the initial movements of grouper eggs we conducted two preliminary simulations using the optional buoyancy algorithm in CMS. This capability applies the physical properties of particles to simulate their sinking or floating. To do this, it uses Stoke's Law, which relates vertical velocity to the diameter and density of the particle, along with the density and viscosity of the water. However, the water density and viscosity are calculated directly from the hydrodynamic model at the depth location of the particle using temperature and salinity estimates, which are highly variable for the hydrodynamic products used here. Therefore, when using different hydrodynamic products the rate that individuals particles ascend in the water column is highly variable across models. Therefore, to eliminate the possibility that differences in the vertical velocity of simulated eggs might introduce variability across our simulations, we decided not to use the buoyancy module during our dispersal simulations. Instead, we conducted two preliminary simulations with the buoyancy module, one using SABGOM and one using HYCOM. We then used the combined results to develop a realistic vertical distribution of grouper eggs during the first two days and applied it to all other simulations. In this way, we were able to use two different hydrodynamic models to realistically approximate the rate that grouper eggs float to the surface, but also use the same rate of vertical movement consistently across all simulations.

We also conducted an additional set of preliminary simulations to investigate whether the rate of egg floating in the first two days is likely to influence our results. Using both SABGOM and HYCOM, we conducted paired simulations that either simulated the eggs floating quickly (reaching the surface 4 hours after release) or remaining uniformly distributed in the water column for the entire first 48 hours. For scamp, we found that whether eggs float quickly or do not float at all has little influence on the findings of our connectivity simulations. Therefore, we used the vertical movement rates derived from the pooled buoyancy simulations described above and applied it consistently to all dispersal simulations.

Vertical Distribution of Larvae

After two days, when grouper eggs typically hatch into larvae (Roberts and Schlieder 1983, Colin et al. 1996), the simulated larvae are subject to vertical migration with depths determined probabilistically from empirical data. For the Base simulation, we used one vertical distribution throughout the entire pelagic larval duration (Table 2) and calculated it using data from ichthyoplankton surveys in the region that operate during the scamp spawning season. Specifically, we analyzed data from surveys that use the Multiple Opening and Closing and Environmental Sensing System (MOCNESS), which holds nine nets and allows scientists to choose the sample depth bin for each net. As a result, the system can sample nine different depth bins in a single tow. Because grouper larvae are rare in the samples, and hard to identify to species, we used data from tows that caught any Epinephelinae larvae during the scamp spawning season. This included 54 larvae caught during Southeast Area Monitoring Assessment Program (SEAMAP) winter surveys (February and March; G. Zapfe, unpublished data) and 18 larvae caught in spring surveys (May) that are independent from SEAMAP (T. Gerard, unpublished data).

For those tows that caught Epinephelinae larvae anywhere in the water column we calculated the mid-depth and density of larvae by volume of water filtered for each depth bin sampled. We organized all of the samples, including those that did not catch any larvae, into 20-meter depth bins from 0 (the surface) to 100 meters, by the mid-depth of the sample. Then, we calculated the mean larval density of the samples in each 20-meter depth bin and used these densities to calculate the proportion of larvae expected in each depth bin. This provides the best estimate of the vertical distribution of scamp larvae, and is what we assumed throughout the entire pelagic larval duration for the base simulation as well as the sensitivity simulations that use different hydrodynamic models (Table 2). CMS uses this user-defined distribution to specify the depth distribution of simulated larvae during each time step.

For the sensitivity simulation that investigated uncertainty in the vertical distribution of larvae we also estimated how this distribution changes with ontogeny. Specifically, we estimated two different vertical distributions, one for pre-flexion larvae and one for post-flexion larvae. The exact timing of flexion is not known for scamp, but closely related grouper species tend to complete flexion at approximately 6 mm in length and 15 days after fertilization (Colin et al. 1996). Therefore, when analyzing MOCNESS data, we used 6 mm to estimate what proportion of pre-flexion and post-flexion grouper larvae in each depth bin. Not all the larvae caught in MOCNESS sampling are measured for length, however, so to obtain large enough sample sizes we had to include grouper larvae from the entire year instead of only the scamp spawning season. Then, we applied these estimates to the vertical distribution of larvae caught during the scamp spawning season (described above) to approximate vertical distributions of pre-flexion and post-flexion scamp larvae. During the sensitivity simulation that includes an ontogenetic shift in vertical distribution (OVM), simulated larvae transition from the pre-flexion distribution to the post-flexion distribution at 15 days after release (Table 2). This approach assumes that the proportion of pre-flexion and post-flexion larvae in each depth bin is relatively consistent across grouper species and seasons. But given the data limitations, it still allows us to consider how variation in ontogenetic vertical migration influences our results.

Text S5 – Pelagic Larval Duration

Because the pelagic larval duration of scamp is unknown, we estimated the competency period of 33 to 52 days as 2.5% and 97.5% quantiles for the ages of newly settled gag grouper larvae. We used the "digitize" package in R (Poisot 2011) to extract the ages of newly settled gag larvae from published reports of gag settlement in the northeastern Gulf of Mexico (Fitzhugh et al. 2005) and the U.S. South Atlantic (Adamski et al. 2012). There is some evidence, however, that gag pelagic larval durations are longer in the Atlantic (Figure S8), so one of our biological ensemble simulations extended the competency period to 57 days, the 97.5% quantile for gag settlement age in the Atlantic.

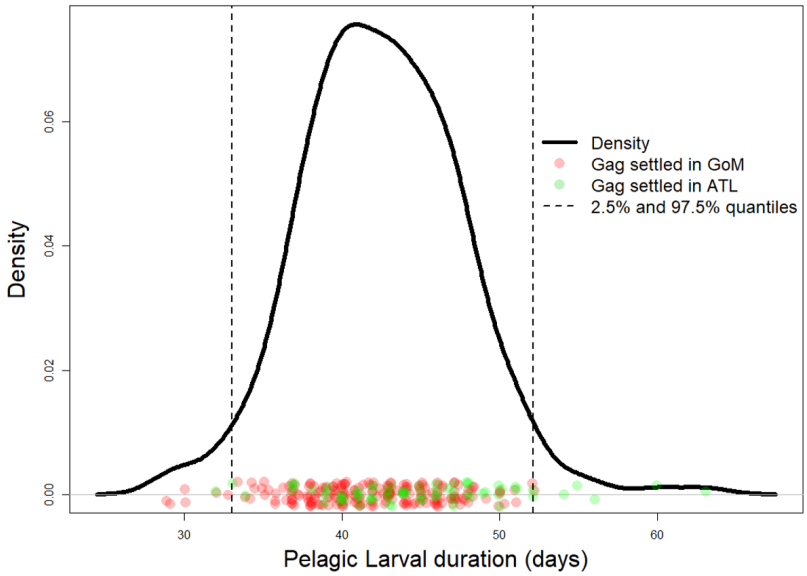

Figure S8: The pelagic larval duration of gag larvae in the Gulf of Mexico and U.S. Atlantic. We allowed simulated larvae to settle between days 33 and 52 (dashed lines), because most gag larvae settle between these ages. Gag larvae in the Atlantic (green points) settle slightly later than those in the Gulf of Mexico, however. Therefore, we conducted a sensitivity simulation that allowed larvae to settle up to 57 days (the 97.5% quantile of Atlantic gag settlement age).

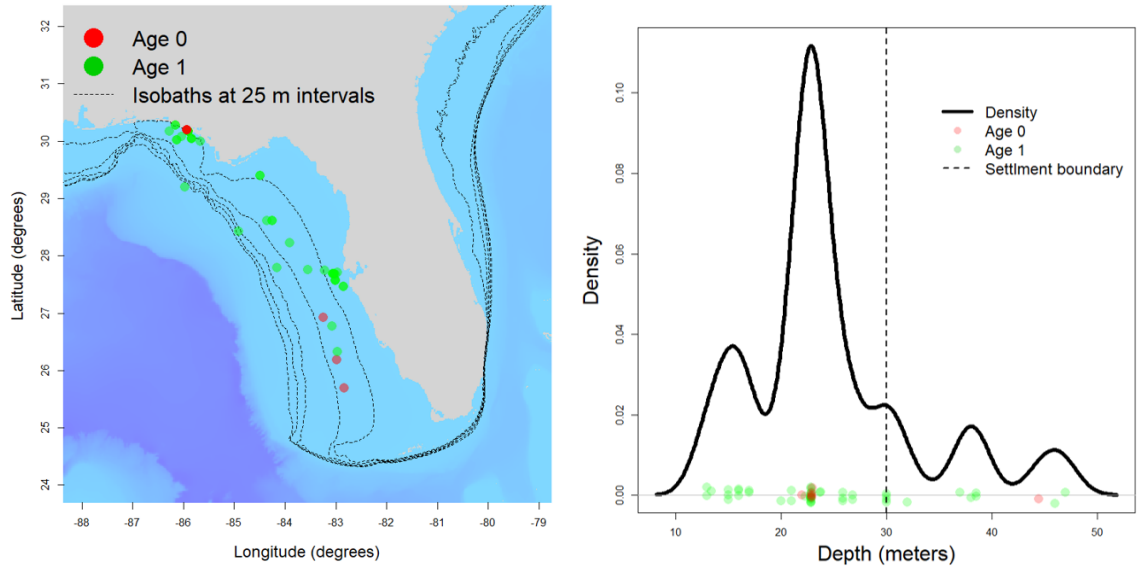

Figure S9: Catch location and depth of age 0 and 1 scamp. Catch locations and associated depths for 47 age 1 and 7 age 0 scamp caught by surveys in the Gulf of Mexico. Although there are few samples, most young scamp were caught in depths less than 30 meters, as is consistent with anecdotal reports in the literature (Coleman et al. 2011). Because data are limited, and the nursery habitat of scamp is uncertain, we investigated two alternative assumptions that allowed virtual larvae to settle at any location with a bottom depth shallower than 30 meters or 45 meters.

Text S6 – Hydrodynamic Products

In total, we used velocity fields from six hydrodynamic products (Table 2), but one was only used as a nest for others that did not cover our entire study area. They came from different ocean circulation models as well as implementations with a range of spatial and temporal resolutions, forcings, and data assimilation approaches.

The GOM HYCOM (1/25°) is a hindcast with 27 vertical layers. It is forced by winds and surface fluxes from the Navy Operational Global Atmospheric Prediction System, large-scale model fields from the HYCOM GOFS at the open boundaries, and data assimilation through the Navy Coupled Ocean Data Assimilation (NCODA) system. The GOM HYCOM HiRes (1/50°) is a data assimilative hindcast simulation with 32 vertical layers. It is forced by daily river discharges implemented at 22 major river discharge points into the Gulf of Mexico and minor river discharge points represented by climatological values. It assimilates satellite observed altimetry and sea surface temperature data as well as salinity and temperature measurements from Argo drifters and Expendable BathyThermographs. The HYCOM GOFS provides forcing at the open boundaries and the surface is forced by atmospheric circulation estimates from the European Centre for Medium-Range Weather Forecasts (ECMWF, 1/8º).

The HYCOM IAS (1/32°) is also a data assimilative hindcast, but it has 30 vertical layers and uses different forcing. The surface is forced by the Climate Forecast System Reanalysis and it includes river inflow by using monthly climatological river discharge to specify a virtual salinity flux. It assimilates satellite observed altimetry and sea surface temperature data as well as salinity and temperature measurements from Argo drifters. The Mercator GLORYS version 12v1 (1/12°) has 50 vertical layers and is a reanalysis from the Copernicus Marine Environment Monitoring Service (Lellouche et al. 2018, Lellouche et al. 2021). It uses version 3.1 of the Nucleus for European Modelling of the Ocean model, driven at surface by ECMWF ERA-Interim reanalysis. It assimilates satellite observed sea level anomaly, sea surface temperature, and sea ice concentration data as well as *in situ* temperature and salinity vertical profiles from the Coriolis Ocean Database ReAnalysis (Lellouche et al. 2018). The SABGOM model implementation (1/25°) has 36 vertical layers and is based on the Regional Ocean Modeling System. The model uses the HYCOM GOFS for open boundary conditions and superimposes tidal harmonics from the ADCIRC western Atlantic tidal database. The surface is forced by the NCEP North American Regional Reanalysis and major rivers in the region are implemented using daily stream flow data from USGS gauges.

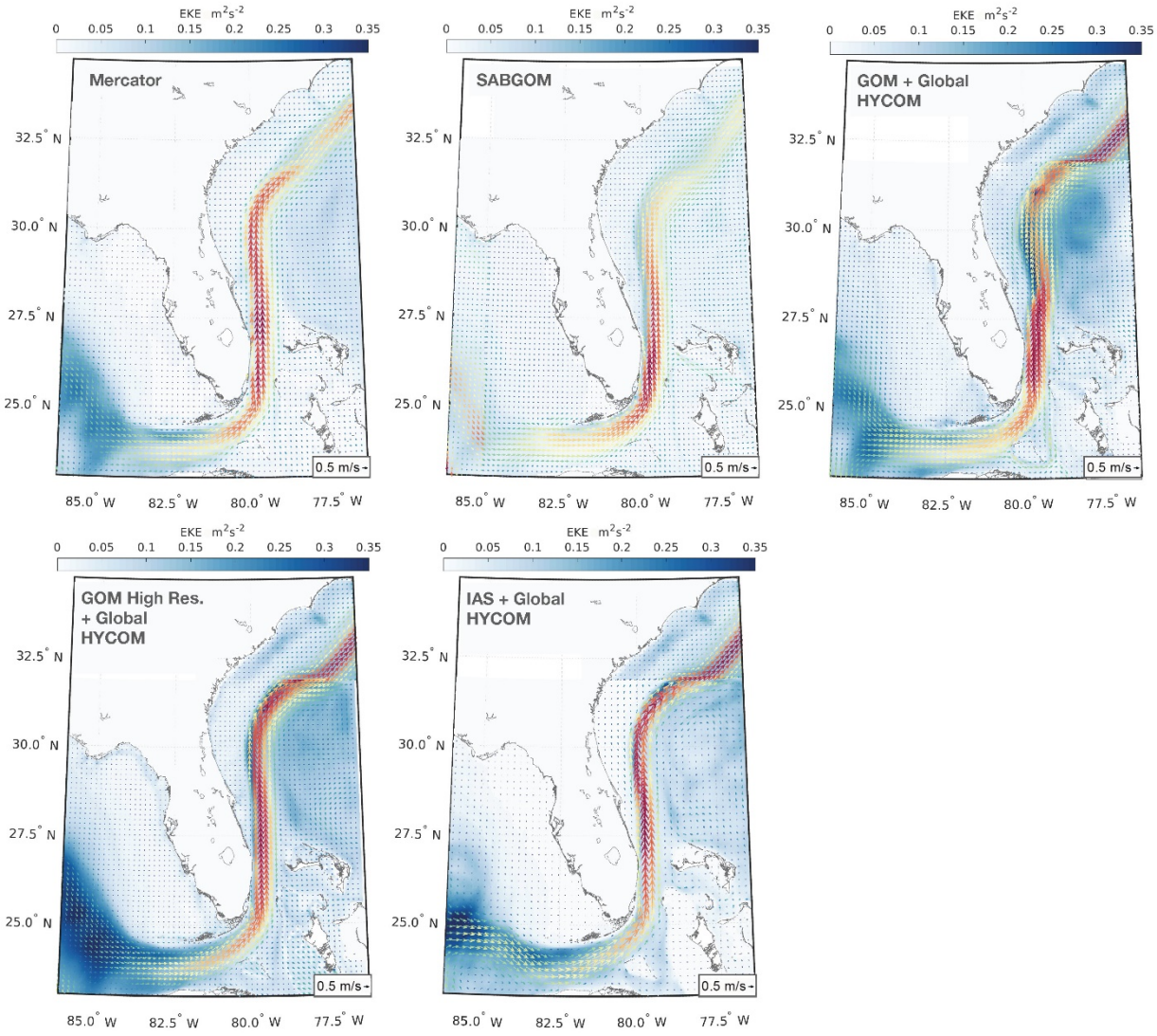

Figure S10: Average eddy kinetic energy (EKE) and current velocity for the velocity fields used in our simulations. Note that these five velocity fields use estimates from six different oceanographic models, but one is only used as a nest for others that do not cover the entire region of interest.

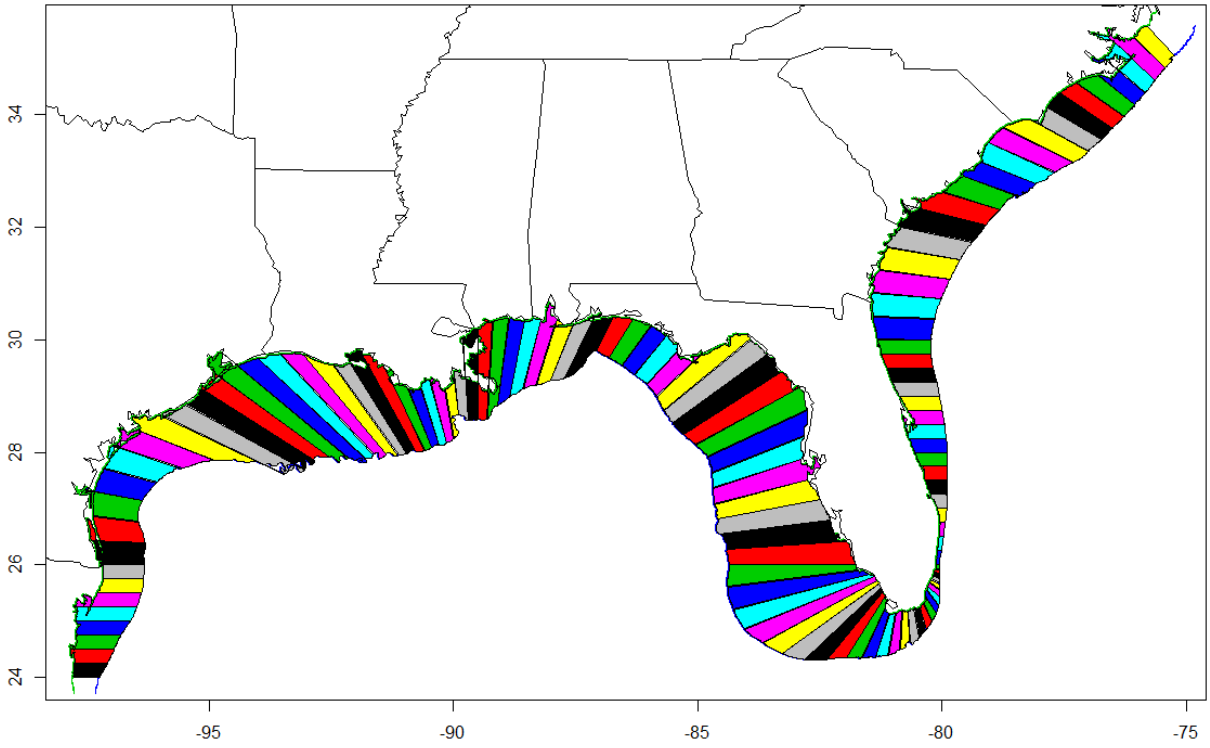

Figure S11: Spatial polygons used to calculate connectivity matrices. These are the spatial polygons used to aggregate successfully settled larvae when calculating connectivity matrices (Figures 2 and S12).

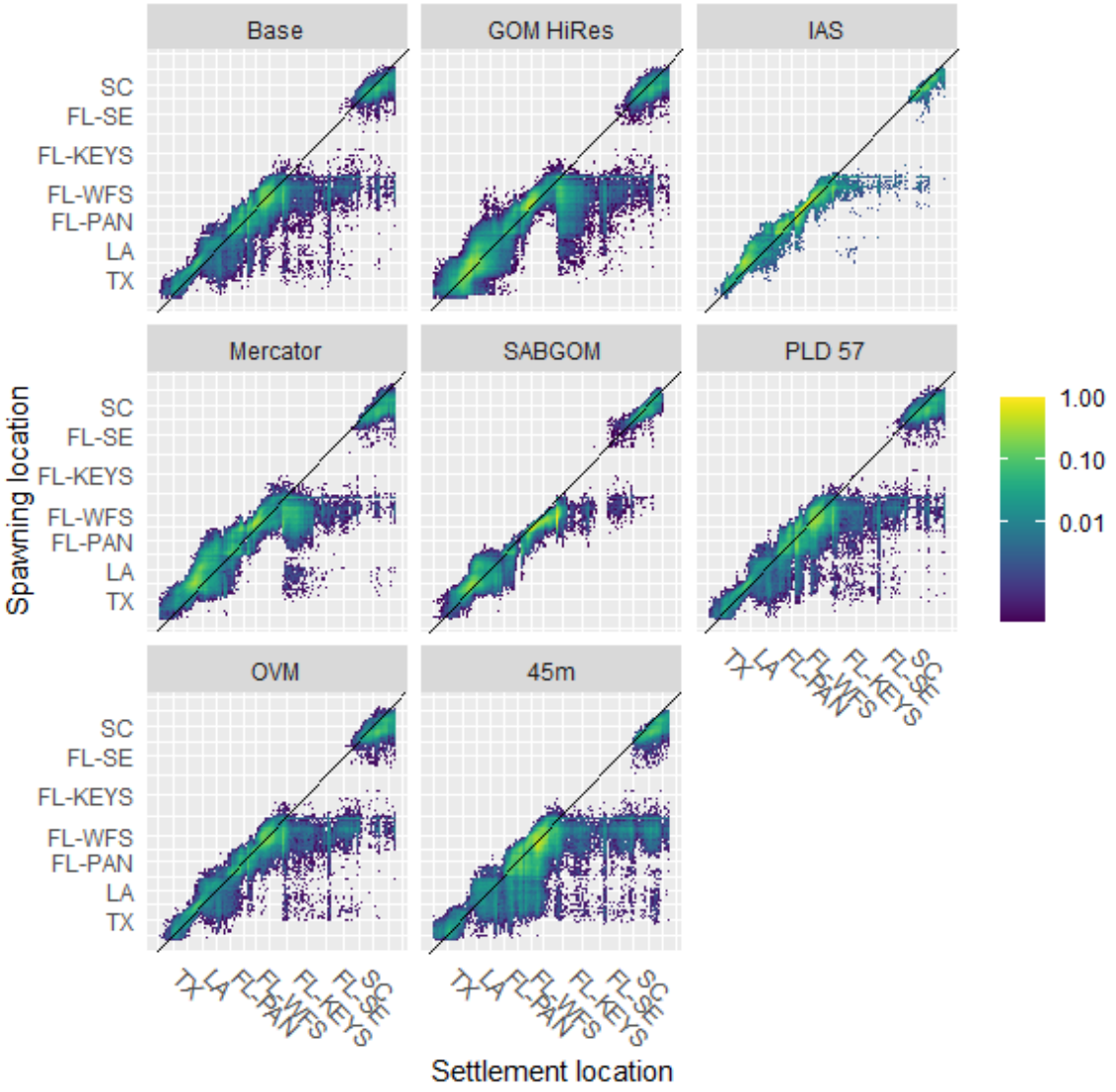

Figure S12: Connectivity matrices by simulation. The vertical axis represents the spawning location, and the horizontal axis represents shows the settlement location of successful virtual larvae. The values (on a log scale) are proportional to the maximum connectivity across all panels with yellow indicating high estimated connectivity and purple indicating low estimated connectivity. The black diagonal line represents the axis of local retention (i.e., settlement location = spawning location). TX = Texas, LA = Louisiana, FL-Pan = the Florida Panhandle, FL-WFS = the West Florida Shelf, FL-Keys = the Florida Keys, FL-SE = the Atlantic coast of Florida, SC = South Carolina. These geographic sub-regions follow the U.S. coastline from west to east and are identified in figure S7.

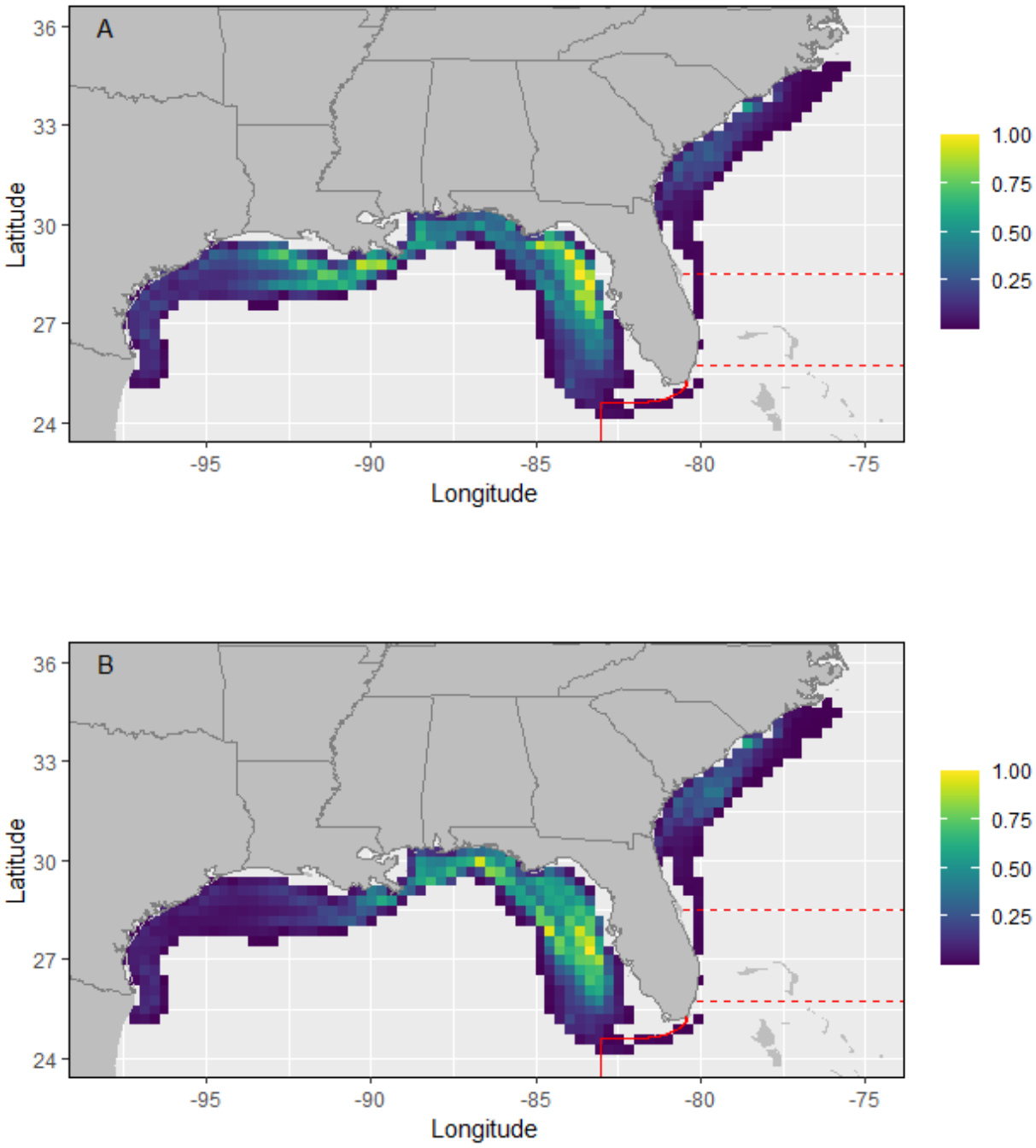

Figure S13: Spawning locations of successful recruits for the hydrodynamic (A) and biological (B) ensembles. Values are proportional to the maximum, with yellow indicating an area where many successful virtual were spawned, and purple indicating an area where few successful particles were spawned.

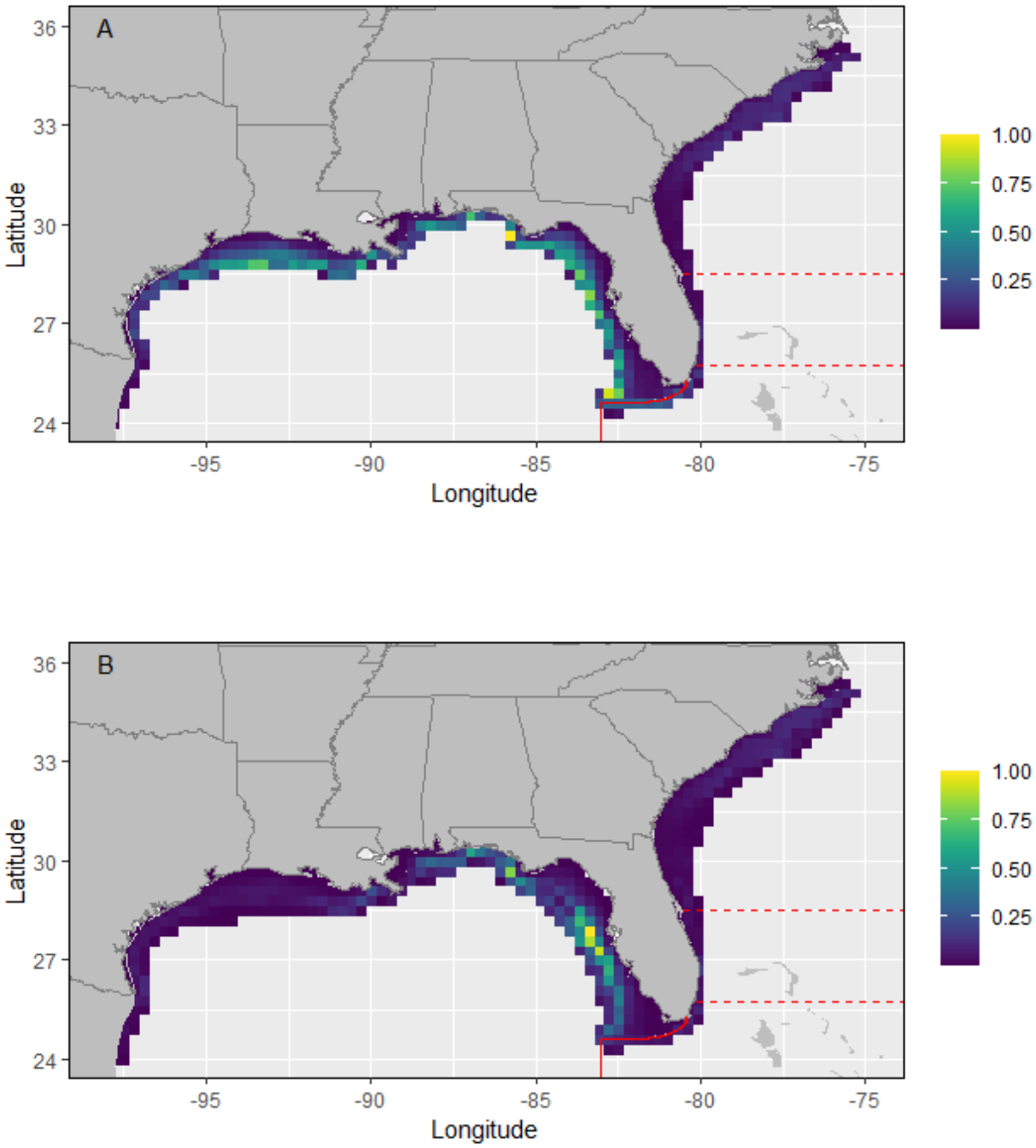

Figure S14: Settlement locations of successful recruits for the hydrodynamic (A) and biological (B) ensembles. Values are proportional to the maximum, with yellow indicating an area where many successful virtual settled, and purple indicating an area where few successful particles settled.

Literature Cited

Adamski KA, Buckel JA, Martin GB, Ahrenholz DW, Hare JA (2012) Fertilization dates, pelagic larval durations, and growth in gag (Mycteroperca microlepis) from North Carolina, USA. Bull Mar Sci 88: 971–986 https://doi.org/10.5343/bms.2012.1003

Bacheler NM, Shertzer KW (2015) Estimating relative abun dance and species richness from video surveys of reef fishes. Fish Bull 113: 15–26 10.7755/FB.113.1.2

Campbell MD, Pollack AG, Gledhill CT, Switzer TS, DeVries DA (2015) Comparison of relative abundance indices calculated from two methods of generating video count data. Fish Res 170: 125–133 https://doi.org/10.1016/j.fishres.2015.05.011

Coleman FC, Scanlon KM, Koenig CC (2011) Groupers on the edge: shelf edge spawning habitat in and around marine reserves of the northeastern Gulf of Mexico. Prof Geogr 63: 456–474 https://doi.org/10.1080/00330124.2011.585076

Colin PL, Koenig CC, Laroche WA (1996) Development from egg to juvenile of the red grouper (Epinephelus morio) (Pisces: Serranidae) in the laboratory. In: Arreguín-Sánchez F, Munro JL, Balgos MC, Pauly D (eds) Biology, fisheries and culture of tropical groupers and snappers. International Center for Living Aquatic Resources Management, Manila, p 399–414

Fitzhugh GR, Koenig CC, Coleman FC, Grimes CB, Sturges WS III (2005) Spatial and temporal patterns in fertilization and settlement of young gag (Mycteroperca microlepis) along the West Florida Shelf. Bull Mar Sci 77: 377–396

Lellouche J, Greiner E, Le Galloudec O, Garric G and others (2018) Recent updates to the Copernicus Marine Service global ocean monitoring and forecasting real-time 1/12° high-resolution system. Ocean Sci 14: 1093–1126 https://doi.org/10.5194/os-14-1093-2018

Lellouche J, Greiner E, Bourdallé-Badie R, Garric G and others (2021) The Copernicus global 1/12° oceanic and sea ice GLORYS12 reanalysis. Front Earth Sci 9: 698876 https://doi.org/10.3389/feart.2021.698876

Marra G, Wood SN (2011) Practical variable selection for generalized additive models. Comput Stat Data Anal 55: 2372–2387 https://doi.org/10.1016/j.csda.2011.02.004

Poisot T (2011) The digitize package: extracting numerical data from scatterplots. R J 3: 25–26 https://doi.org/10.32614/RJ-2011-004

Roberts DE, Schlieder RA (1983) Induced sex inversion, mat uration, spawning and embryogeny of the protogynous grouper, Mycteroperca microlepis. J World Maric Soc 14: 639–649

Schobernd ZH, Bacheler NM, Conn PB (2014) Examining the utility of alternative video monitoring metrics for indexing reef fish abundance. Can J Fish Aquat Sci 71: 464–471 https://doi.org/10.1139/cjfas-2013-0086